Special Section: Consumer Technology-Based Solutions for COVID-19

Crowd Size Estimation Using CommSense Instrument for COVID-19 Echo Period

Santu Sardar
IIT Hyderabad

Mohammed Z. A. Khan
IIT Hyderabad

Amit K. Mishra
University of Cape Town

***Abstract*—The period after the COVID-19 wave is called the Echo-period. Estimation of crowd size in an outdoor environment is essential in the Echo-period. Making a simple and flexible working system for the same is the need of the hour. This article proposes and evaluates a nonintrusive, passive, and cost-effective solution for crowd size estimation in an outdoor environment. We call the proposed system as LTE communication infrastructure based environment sensing or LTE-CommSense. This system does not need any active signal transmission as it uses LTE transmitted signal. So, this is a power-efficient, simple, low-footprint device. Importantly, the personal identity of the people in the crowd cannot be obtained using this method. First, the system uses practical data to determine whether the outdoor environment is empty or not. If not, it tries to estimate the number of people occupying the near range locality. Performance evaluation with practical data confirms the feasibility of this proposed approach.**

With the outbreak of COVID-19 virus, we are forced to rethink visiting public areas[1–4]. After the current primary wave of infection improves, we will be living in a period when we will need to run business "almost" as usual without a vaccine. This phase is sometimes called the Echo-period.[5] In this scenario, a device to measure the crowd size is urgently required. Crowd sensing is an active area of research because of its diverse applications.

Digital Object Identifier 10.1109/MCE.2020.3032791
Date of publication 21 October 2020; date of current version 2 February 2021.

Keeping this in mind, a passive system, called CommSense (communication-based environment sensing system), is proposed here for measuring crowd size in an outdoor environment. The concept of CommSense was proposed and verified by the authors in simulation and with field-collected data for various indoor applications, such as indoor object detection, indoor localization, and indoor occupancy estimation.[6] The system was also tested for outdoor vehicle detection and classification.[7] These give the confidence to apply the CommSense principle. A major advantage of the CommSense system, compared to audio or vision-based methods, is that our system is nonintrusive. It cannot identify the persons.

The experiments and analyses performed here are as follows.

1) First, we considered that the people in the outdoor crowd are static. Crowd detection using a threshold-based method was performed first. If a crowd is detected, it triggers the investigation of the deriving number of persons in the crowd.
2) In the next step, the same analysis was repeated when the people in the crowd were moving freely.
3) Finally, we have performed these two experiments on a different day and time to examine the consistency of this approach.

STATE OF THE ART

As crowd sensing is vital for many other applications,[8,9] there have been attempts to perform outdoor-crowd-size estimation in the past. Video-based crowd-size estimation was proposed by Li *et al.*[10] The performance of video processing for crowd-monitoring applications was analyzed by Bailas *et al.*[11] A crowd-counting method was proposed by Xing *et al.*,[12] which uses detection flow along the temporal video sequence. Automated video analytic was used for crowd monitoring and counting in the work by Cheong *et al.*[13] Counting the number of people present in a crowd with a real-time network of image sensors was proposed by Yang *et al.*[14]. A motion-based crowd density estimation method was proposed by Chondro *et al.*[15] A crowd-counting method based on image processing and convolutional neural network was proposed by Liu *et al.*[16] But these vision-based approaches require the crowd to be in the line-of-sight of the cameras. Their performance also depends on the overlapping of the objects, the relative positioning of the crowd, visibility at the time of the day, weather conditions, pollution level, etc. Additionally, it also poses privacy concerns. Danielis *et al.*[17] tried to estimate the size of dense crowds, using a distributed protocol that relies on mobile device-to-device communication. This required active transmission at all times and was verified in simulation. In addition, we need crowd-size estimation on a smaller scale. Khan *et al.*[18] use smartphones' acoustic sensors in the presence of human conversation, and motion sensors in the absence of any conversational data, for crowd-size estimation. There has been few attempts to use LTE-based systems for crowd-density estimation.[19,20] Tripathy *et al.*[21] presented an Internet-of-Medical-Things-enabled wearable called EasyBand for autocontact tracing. Currently, the world is almost coming to a halt to reduce COVID-19 spread. Official recommendations for social distancing have pushed people into ever-smaller clusters.[1]

LTE-CommSense SYSTEM

Figure 1(a) shows a simple version of the proposed system that uses a piece of single user equipment (UE).[6,7] In this article, a single UE was considered for verification using practical data. The LTE UE receiver works at Band-40 (2300–2400-MHz frequency band) in time division duplexing topology. The signal captured had a bandwidth of 10 MHz.

In the experimental setup, we have used a total of 19 number of people in an outdoor roadside environment. The CommSense prototype was employed to collect LTE downlink (DL) data affected by the presence of the crowd. The modeled UE, which is a part of the proposed prototype, then receives the DL data and performs standard UE operations to evaluate state information (CSI).

The description and working principle of an USRP N200 SDR platform can be obtained from the work by Sardar *et al.*[6,7] The SDR was modeled as the CommSense prototype containing LTE receiver. The LTE DL signal was captured via the antenna and radio frequency (RF) daughter card

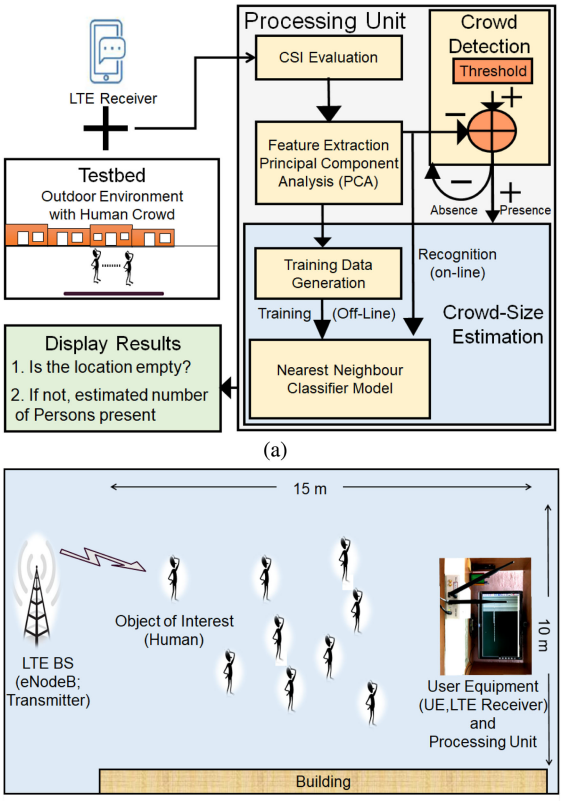

Figure 1. (a) Block diagram of LTE-CommSense system that uses a single UE for outdoor crowd-size estimation. (b) Relative position of LTE receiver, crowd, and LTE eNodeB in the outdoor environment.

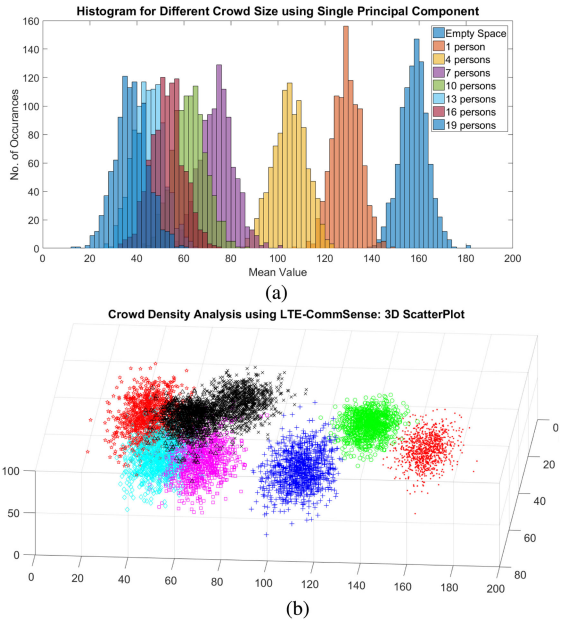

Figure 2. Static crowd detection. (a) Histogram of principal component for largest eigenvalue. (b) Scatterplot corresponding to highest three eigenvalues.

connected to the N200 platform. Figure 1(b) explains the relative position of the prototype, crowd, and LTE base station (eNodeB) in the outdoor environment in the experimental setup. First, the LTE DL data were recorded without the presence of the crowd, and then for different numbers of people present. This method is performed for two scenarios. In one case, the persons in the crowd are static, and in another case, they were moving without any restriction within the premises. For each DL data capture, a thousand CSI values were extracted.

CASE STUDY DESIGN

Detection for Static and Dynamic Crowd

As per the experimental setup, there are a total of eight different cases. The first class corresponds to the outdoor environment with the absence of any crowd. The next category denotes the presence of only one person. Category three is for the presence of four persons. In a similar manner, we keep on increasing the number of persons by 3 until the 8th category corresponding to the presence of 19 persons was reached. For all these eight categories, 1000 CSI values were extracted. Now, to detect the presence of a person, principal component analysis (PCA) was performed for feature extraction of the CSI values.[6]

Principal components for all the categories corresponding to the largest eigenvalue are plotted in Figure 2(a). Figure 2(b) depicts the three-dimensional scatterplots of the principal components for the largest three eigenvalues. The description of the categories for Figure 2(b) is explained in Table 1. In this plot, distinguishable clusters are visible corresponding to the absence of crowd and the presence of different sizes of the crowd. In Figure 2(a), for the case where only one principal component corresponding to the largest eigenvalue was considered, the overlap between the clusters was more, and this overlap decreases gradually when more number of principal components were considered.

Table 1. Category Description in the Three-Dimensional Clusterplot for Three Principal Components corresponding to Highest Three Eigenvalues.

Symbol	Experiment Description	Category
●	Empty Outdoor Environment	1
○	No. of Persons = 1	2
+	No. of Persons = 4	3
X	No. of Persons = 7	4
□	No. of Persons = 10	5
◇	No. of Persons = 13	6
△	No. of Persons = 16	7
★	No. of Persons = 19	8

The aforementioned analysis was performed next when the persons were in random motion in the locality. Principal components for all the categories corresponding to the largest eigenvalue are plotted in Figure 3(a). Figure 3(b) depicts the three-dimensional scatterplots of the principal components for the largest three eigenvalues. The description of the categories for Figure 3(b) is same as in Table 1. In this plot, distinguishable clusters are visible corresponding to the absence of crowd and the presence of different sizes of the crowd. In Figure 3(a), i.e., for the case where only one principal component

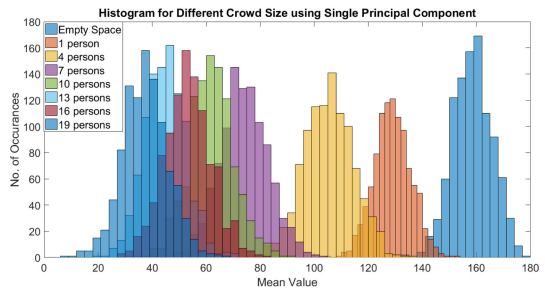

(a)

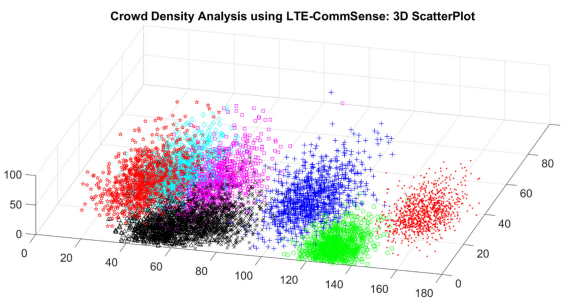

(b)

Figure 3. Dynamic crowd detection. (a) Histogram of principal component for largest eigenvalue. (b) Scatterplot corresponding to highest three eigenvalues.

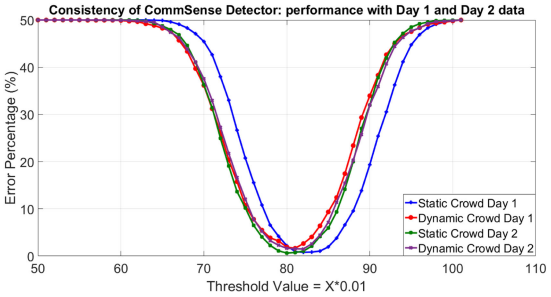

Figure 4. Consistency of CommSense detector performance: Comparison of detection performance at two different days.

corresponding to the largest eigenvalue was considered, the overlap between the clusters was more.

Threshold-Based Detection and Verification of Consistency

Threshold-based detection performance corresponding to different values of the selected threshold may be analyzed for both static and dynamic case. For static crowd, as shown in Figure 2(a), the error percentage of crowd detection versus the selected threshold was shown in Figure 4. The percentage of error in detection was obtained to be 0.65% for a threshold value of 0.80. The same analysis was performed for the dynamic crowd shown in Figure 3(a). The error percentage of 1.7% was evaluated for a threshold value of 0.82 [see Figure 2(d)]. Both these results are depicted in Figure 4, labeled as "Static Crowd Day 1" and "Dynamic Crowd Day 1," respectively.

We evaluated the performance consistency of the proposed approach to ascertain the reliability of the developed prototype. The exercise was repeated on a different day with a new set of people. In Figure 4, we can see the detection performance for the other day (Day 2) was also along with the initial day data. In "Day 2," for these two different types of crowds, minimum detection errors achieved a minimum value of 0.8% and 1.55%, respectively. Comparison with the performances of Day 1 concludes that both the days' detection performance was consistent.

Estimation of Crowd Size for Static and Dynamic Crowd

Detection of the crowd triggers the next stage of analysis. Here, we attempt to estimate crowd

Table 2. Classification of Number of Persons Present for Static and Dynamic Crowd Scenario.

Training images	Testing images	Accuracy (%) for static crowd	Accuracy (%) for dynamic crowd
200	250	85.9	84.35
300	350	86.3	85.36
400	500	86.02	84.55
500	700	85.3	83.02
600	800	85.6	83.72
750	1000	85.6	83.91

Table 3. Confusion Matrix for Static and Dynamic Crowd for the Case of 500 Training Data per Category and 700 Testing Data per Category.

Static Crowd							
697	3	0	0	0	0	0	0
1	698	1	0	0	0	0	0
0	1	699	0	0	0	0	0
0	0	0	682	7	0	11	0
0	0	0	7	671	15	5	2
0	0	0	0	29	644	1	26
0	0	0	8	7	0	685	0
0	0	0	1	2	26	1	670
Dynamic Crowd							
697	3	0	0	0	0	0	0
1	685	14	0	0	0	0	0
0	10	688	2	0	0	0	0
0	0	3	659	22	1	14	1
0	0	5	12	639	28	14	2
0	0	0	0	24	623	5	48
0	0	0	11	11	10	658	10
0	0	0	0	1	44	5	650

size, i.e., the number of persons in the crowd. Table 2 depicts the evaluated accuracy for different numbers data for training and size estimation. A simple nearest neighbor classifier was chosen for this purpose. When new sample data are input to the system, using the nearest neighbor classifier the distance of that from the nearest data available in the training dataset was evaluated. The results reveal that the proposed approach is a promising candidate for crowd detection and its size estimation in an outdoor environment consisting of either static or dynamic persons present in the crowd. Table 3 shows the confusion matrix for the lowest accuracy achieved in Table 2. The corresponding accuracy achieved for the static and dynamic crowd cases are 86.02% and 84.55%, respectively.

CONCLUSION

This article proposes a passive nonintrusive solution for outdoor crowd detection and subsequently, its size estimation. The feasibility of this novel approach was verified with practical signal captured using SDR-based prototype developed by the authors. The results prove the feasibility of our proposal.

Consistency of the performance of this proposal was evaluated by calculating the detection accuracy for static and dynamic crowd on a different day with a different set of people. Similar performance was observed, which proves the performance consistency.

For the static as well as dynamic crowd cases, the nearest neighbor classifier provided acceptable performance.

The analysis in this article with practical data confirms that LTE-CommSense principle can successfully detect crowd in outdoor environment. After detection, it can estimate the crowd size as well with reasonable accuracy.

REFERENCES

1. V. S. Rathore, V. Kumawat, and B. Umamaheswari, "Coronavirus (COVID-19) in India—Statistics &facts," in *Proc. 4th World Conf. Smart Trends Syst., Secur., Sustainability*, 2020, pp. 518–521.
2. T. Coughlin, "Impact of COVID-19 on the consumer electronics market," *IEEE Consum. Electron. Mag.*, to be published, doi: 10.1109/MCE.2020.3016753.
3. R. Abbas and K. Michael, "COVID-19 contact trace app deployments: Learnings from Australia and Singapore," *IEEE Consum. Electron. Mag.*, vol. 10, no. 5, pp. 65–70, Sep. 2020.
4. K. Michael and R. Abbas, "Behind COVID-19 contact trace apps: The Google–Apple partnership," *IEEE Consum. Electron. Mag.*, vol. 9, no. 5, pp. 71–76, Sep. 2020.
5. "Multilateral call for solutions for COVID-19 echo period - life without a vaccine." 2020. Accessed: Jun. 19, 2020. [Online]. Available: https://www.eurekanetwork.org/content/multilateral-call-solutions-covid-19-echo-period

6. S. Sardar, A. K. Mishra, and M. Z. A. Khan, "Indoor occupancy estimation using the LTE-CommSense system," *Int. J. Remote Sens.*, vol. 41, no. 14, pp. 5609–5619, 2020. [Online]. Available: https://doi.org/10.1080/2150704X.2020.1734246.
7. S. Sardar, A. K. Mishra, and M. Z. A. Khan, "Vehicle detection and classification using LTE-CommSense," *IET Radar, Sonar, Navigation*, vol. 13, no. 5, pp. 850–857, 2019.
8. S. P. Mohanty, U. Choppali, and E. Kougianos, "Everything you wanted to know about smart cities: The Internet of things is the backbone," *IEEE Consum. Electron. Mag.*, vol. 5, no. 3, pp. 60–70, Jul. 2016.
9. A. Baldini *et al.* "Room occupancy detection: Combining RSS analysis and fuzzy logic," in *Proc. IEEE 6th Int. Conf. Consum. Electron.*, Sep. 2016, pp. 69–72.
10. W. Li, X. Wu, K. Matsumoto, and H. Zhao, "A new approach of crowd density estimation," in *Proc. IEEE Region 10 Conf.*, 2010, pp. 200–203.
11. C. Bailas, M. Marsden, D. Zhang, N. E. O'Connor, and S. Little, "Performance of video processing at the edge for crowd-monitoring applications," in *Proc. IEEE 4th World Forum Internet Things*, 2018, pp. 482–487.
12. J. Xing, H. Ai, L. Liu, and S. Lao, "Robust crowd counting using detection flow," in *Proc. 18th IEEE Int. Conf. Image Process.*, 2011, pp. 2061–2064.
13. K. H. Cheong *et al.*, "Practical automated video analytics for crowd monitoring and counting," *IEEE Access*, vol. 7, pp. 183252–183261, 2019.
14. Yang, Gonzalez-Banos, and Guibas, "Counting people in crowds with a real-time network of simple image sensors," in *Proc. 9th IEEE Int. Conf. Comput. Vis.*, 2003, pp. 122–129.
15. P. Chondro, C. Liu, C. Chen, and S. Ruan, "Detecting abnormal massive crowd flows: Characterizing fleeing en masse by analyzing the acceleration of object vectors," *IEEE Consum. Electron. Mag.*, vol. 8, no. 4, pp. 32–37, Jul. 2019.
16. Z. Liu, Y. Chen, B. Chen, L. Zhu, D. Wu, and G. Shen, "Crowd counting method based on convolutional neural network with global density feature," *IEEE Access*, vol. 7, pp. 88789–88798, 2019.
17. P. Danielis, S. T. Kouyoumdjieva, and G. Karlsson, "UrbanCount: Mobile crowd counting in urban environments," in *Proc. 8th IEEE Annu. Inf. Technol., Electron. Mobile Commun. Conf.*, 2017, pp. 640–648.
18. M. A. A. H. Khan, H. M. S. Hossain, and N. Roy, "SensePresence: Infrastructure-less occupancy detection for opportunistic sensing applications," in *Proc. 16th IEEE Int. Conf. Mobile Data Manage.*, 2015, vol. 2, pp. 56–61.
19. M. De Sanctis, T. Rossi, S. Di Domenico, E. Cianca, G. Ligresti, and M. Ruggieri, "LTE signals for device-free crowd density estimation through CSI secant set and SVD," *IEEE Access*, vol. 7, pp. 159943–159951, 2019.
20. S. D. Domenico, M. D. Sanctis, E. Cianca, P. Colucci, and G. Bianchi, "LTE-based passive device-free crowd density estimation," in *Proc. IEEE Int. Conf. Commun.*, May 2017, pp. 1–6.
21. A. K. Tripathy, A. G. Mohapatra, S. P. Mohanty, E. Kougianos, A. M. Joshi, and G. Das, "EasyBand: A wearable for safety-aware mobility during pandemic outbreak," *IEEE Consum. Electron. Mag.*, vol. 9, no. 5, pp. 57–61, Sep. 2020.

Santu Sardar received the Ph.D. degree from IIT Hyderabad in 2020 and is currently the director of a DRDO Laboratory working on quantum technologies. Contact him at sardar.santu@gmail.com.

Amit K. Mishra is a Professor in Radar Remote Sensing Group at the Univeristy of Cape Town. His areas of interest includes radar signal processing and applied AI. Contact him at akmishra@ieee.org.

Mohammed Z. A. Khan was with Sasken, Silica Semiconductors, and Hellosoft. He is currently a professor with IIT Hyderabad, Kandi, India. His contributions in space–time block codes are adopted by the WiMAX Standard. Contact him at zafar@iith.ac.in.